

# Universal Decomposition of the Low-Frequency Conductivity Spectra of Iron-Pnictides Uncovering Fermi-Liquid Behavior

D. Wu,<sup>1</sup> N. Barišić,<sup>1</sup> P. Kallina,<sup>1</sup> A. Faridian,<sup>1</sup> B. Gorshunov,<sup>1</sup> N. Drichko,<sup>1</sup>  
L. J. Li,<sup>2</sup> X. Lin,<sup>2</sup> G. H. Cao,<sup>2</sup> Z. A. Xu,<sup>2</sup> N. L. Wang,<sup>3</sup> and M. Dressel<sup>1</sup>

<sup>1</sup>*Physikalisches Institut, Universität Stuttgart, Pfaffenwaldring 57, 70550 Stuttgart, Germany*

<sup>2</sup>*Department of Physics, Zhejiang University, Hangzhou 310027, People's Republic of China*

<sup>3</sup>*Institute of Physics, Chinese Academy of Sciences, Beijing 100190, People's Republic of China*

(Dated: May 31, 2019)

Infrared reflectivity measurements on 122 iron-pnictides reveal the existence of two electronic subsystems. The one gapped due to the spin-density-wave transition in the parent materials, such as  $\text{EuFe}_2\text{As}_2$ , is responsible for superconductivity in the doped compounds, like  $\text{Ba}(\text{Fe}_{0.92}\text{Co}_{0.08})_2\text{As}_2$  and  $\text{Ba}(\text{Fe}_{0.95}\text{Ni}_{0.05})_2\text{As}_2$ . Analyzing the dc resistivity and scattering rate of this contribution, a hidden  $T^2$  dependence is found, indicating that superconductivity evolves out of a Fermi-liquid state. The second subsystem gives rise to incoherent background, present in all 122 compounds, which is basically temperature independent, but affected by the superconducting transition.

PACS numbers: 74.25.Gz, 71.30.+h, 74.25.Gz, 74.25.Jb

In the course of the past year, it became apparent that both the normal and superconducting states of iron-pnictides are more complex than in conventional metals [1, 2]. Understanding their magnetic and structural orders in parallel to superconductivity is one of the main challenges. An additional complication is the presence of several bands close to the Fermi energy where nesting might be crucial for the magnetic order [3, 4]. Substituting Ba by K in  $\text{BaFe}_2\text{As}_2$ , for instance, introduces holes and affects structural and spin density wave (SDW) transitions, which are both suppressed for the benefit of superconductivity [5]. When Co or Ni partially replaces Fe also both transitions are suppressed and superconductivity is observed up to  $T_c = 25$  K [6, 7]. The proximity of a magnetic ground state raises the question about the role of magnetic fluctuations [8], which – together with the observed anomalous transport behavior – evokes a quantum-phase-transition scenario for superconductivity [9, 10]. Here we compare the optical properties on different 122-iron-pnictide compounds and find that the low-frequency conductivity spectra can be universally decomposed into a broad temperature independent part and a narrow zero-frequency contribution. The latter one exhibits a Fermi-liquid behavior and governs the physical behavior of these materials. Single crystals of  $\text{EuFe}_2\text{As}_2$ ,  $\text{Ba}(\text{Fe}_{0.92}\text{Co}_{0.08})_2\text{As}_2$ , and  $\text{Ba}(\text{Fe}_{0.95}\text{Ni}_{0.05})_2\text{As}_2$  were grown using FeAs as self-flux dopants [7, 9] and characterized by X-ray, EDX-microanalysis, transport and susceptibility measurements [Fig. 3(a,b)]. The high reproducibility of the resistivity measurements and the sharp transition observed in the susceptibility indicate that the samples are homogeneously doped [11]. The temperature dependent optical reflectivity (in  $ab$  plane) was measured in a wide frequency range from 20 to 37 000  $\text{cm}^{-1}$  using a series of spectrometers. The low-frequency extrapolation was done according to the dc conductivity mea-

sured on the same crystals. The complex optical conductivity  $\hat{\sigma}(\omega) = \sigma_1(\omega) + i\sigma_2(\omega)$  was calculated from the reflectivity spectra using Kramers-Kronig analysis. In Fig. 1 we present the in-plane optical properties of  $\text{Ba}(\text{Fe}_{0.92}\text{Co}_{0.08})_2\text{As}_2$  and  $\text{Ba}(\text{Fe}_{0.95}\text{Ni}_{0.05})_2\text{As}_2$  at different temperatures. The reflectivity is metallic but does not exhibit a clear-cut plasma edge similar to other 122 iron-pnictide compounds [12, 13, 14, 15, 16, 17, 18]. The optical conductivity contains a broad double-peak in the mid- and near-infrared that does not change considerably with temperature. As  $T$  decreases, a Drude-like contribution develops and becomes narrower. Both features are sep-

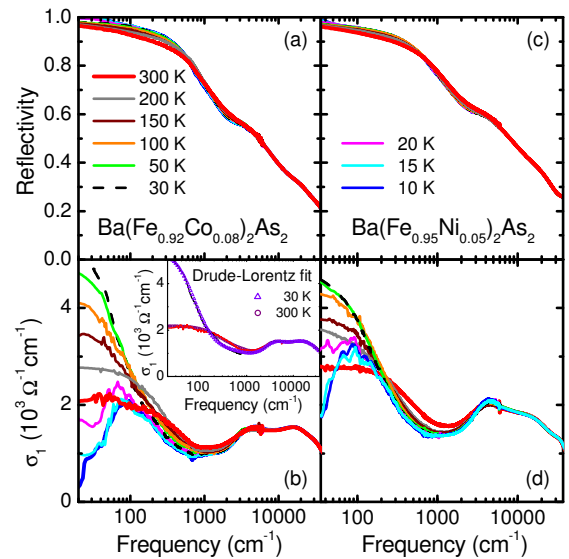


FIG. 1: (Color online) Optical reflectivity and conductivity of  $\text{Ba}(\text{Fe}_{0.92}\text{Co}_{0.08})_2\text{As}_2$  and  $\text{Ba}(\text{Fe}_{0.95}\text{Ni}_{0.05})_2\text{As}_2$  measured at different temperatures between 10 K and 300 K in a wide spectral range. Examples of Drude-Lorentz fits are displayed in the inset for two temperatures  $T = 30$  K and 300 K.

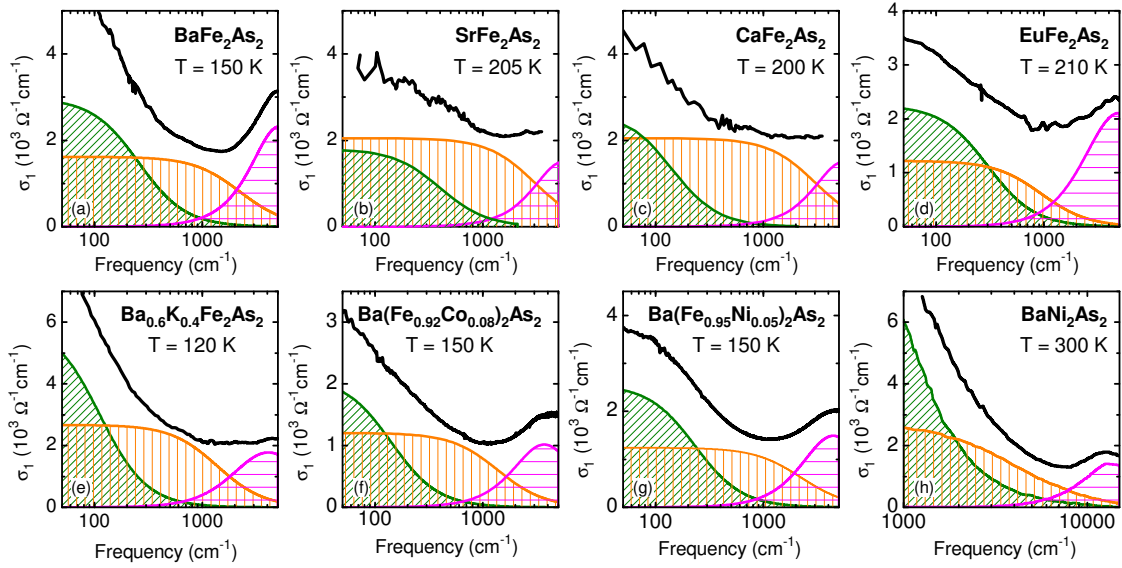


FIG. 2: (Color online) In the metallic state the optical conductivity of different iron-pnictides can always be described by two Drude terms ( $\sigma_N$ -densely shaded green and  $\sigma_B$ -medium shaded orange) and an oscillator in the mid-infrared (sparsely hatched magenta). The spectra of the parent compounds at temperatures above the SDW transition: (a)  $\text{BaFe}_2\text{As}_2$  [12], (b)  $\text{SrFe}_2\text{As}_2$  [12], (c)  $\text{CaFe}_2\text{As}_2$  [13], and (d)  $\text{EuFe}_2\text{As}_2$  [14]. For  $T > T_c$  the conductivity spectra of the electron doped superconductor  $\text{Ba}_{0.6}\text{K}_{0.4}\text{Fe}_2\text{As}_2$  [15], the hole doped superconductors (f)  $\text{Ba}(\text{Fe}_{0.92}\text{Co}_{0.08})_2\text{As}_2$  and (g)  $\text{Ba}(\text{Fe}_{0.95}\text{Ni}_{0.05})_2\text{As}_2$  are very similar. (h) When Fe is completely substituted by Ni, the material is more metallic, but the room-temperature spectrum of  $\text{BaNi}_2\text{As}_2$  [16] can be decomposed in the same way with a larger spectral weight of the Drude components.

arated by a minimum in  $\sigma_1(\omega)$  around  $1000 \text{ cm}^{-1}$ . The parent compound  $\text{EuFe}_2\text{As}_2$  was discussed in Ref. 14. When we try to fit the normal-state spectra by a minimum number of Drude and Lorentz contributions [19], we obtain a satisfactory description only by using two Drude terms [20]. Importantly, this decomposition holds universally for different 122-iron-pnictides. This is illustrated in Fig. 2 where the optical conductivity is displayed in a large frequency range for parent compounds  $X\text{Fe}_2\text{As}_2$  ( $X = \text{Ba}, \text{Sr}, \text{Ca}, \text{Eu}$ ), as well as for hole-doped  $\text{Ba}_{0.6}\text{K}_{0.4}\text{Fe}_2\text{As}_2$  and for the completely substituted  $\text{BaNi}_2\text{As}_2$  [12, 13, 14, 15, 16]. A simple oscillator models the mid-infrared properties sufficiently well. A broad contribution  $\sigma_B$  mimics the considerable background conductivity that seems to be similar for all compounds and does not change appreciably with temperature. As will be discussed later, the distinct properties of the particular material are solely determined by the second Drude term  $\sigma_N$  with a width of approximately  $100 \text{ cm}^{-1}$  in the case of  $\text{Ba}(\text{Fe}_{0.92}\text{Co}_{0.08})_2\text{As}_2$ . Its spectral weight is smaller by a factor of 3-5 compared to  $\sigma_B$ . Upon cooling, the spectral weight is roughly conserved for each of these two subsystems. Our finding is in accord with angle-resolved photoemission (ARPES) data [21] which indicate that the multi-band structure does not change considerably upon doping and temperature. In order to analyze the temperature dependence of  $\sigma_N$  at  $\omega = 0$ , we have measured the dc resistivity [see Fig. 3(a)], then simply deduce a constant

$\sigma_B$  from the graphs displayed in Fig. 2 and consider  $\sigma_N(T) = \sigma_{\text{total}}(T) - \sigma_B$ . The result is surprising but very simple, namely  $\rho_N = 1/\sigma_N \propto T^2$  over the broad temperature range, as shown in Fig. 3(c). Such a temperature dependence is a clear sign of Fermi liquid behavior. Importantly, an independent confirmation of this finding is obtained directly from the decomposition of the low-frequency conductivity of  $\text{Ba}(\text{Fe}_{1-x}\text{M}_x)_2\text{As}_2$ . The Drude fit  $\sigma_N(\omega) = \sigma_N(\omega = 0)/(1 + \omega^2\tau_N^2)$  yields a scattering rate  $1/\tau_N(T) \propto T^2$  as well [Fig. 3(d)]. These results evidence a deep physical consistency of our decomposition. We want to point out that due to the broad frequency range covered by only two Drude contributions, the fits are robust and give well defined parameters  $\sigma_B$ ,  $\sigma_N(T)$ , and  $1/\tau_N(T)$ . Furthermore, we restrain ourselves by assuming  $\sigma_B$  basically as temperature independent; and since the dc-conductivity is determined separately, that leaves only  $1/\tau_N(T)$  as a fit parameter. Moreover, as a result of such fit procedure it turns out that the coherent Drude term preserves its spectral weight within an uncertainty of 2%. The fact that the plasma frequency does not change much with temperature reinforces the conclusion that the coherent Drude describes a classical Fermi liquid. Our findings are in agreement with the conclusion drawn from a comprehensive Hall-effect study on the series  $\text{Ba}(\text{Fe}_{1-x}\text{Co}_x)_2\text{As}_2$  [22] indicating that the iron-pnictides are good Fermi liquids. As discussed there the values of scattering rate and the  $T^2$  behavior agree reasonably with the weak coupling limit under assump-

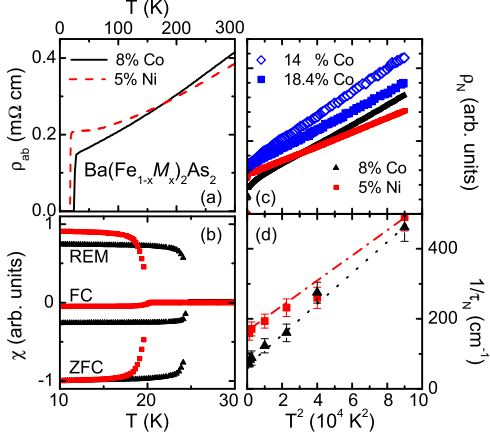


FIG. 3: (Color online) (a) Temperature dependence of the electrical resistivity of  $\text{Ba}(\text{Fe}_{0.92}\text{Co}_{0.08})_2\text{As}_2$  and  $\text{Ba}(\text{Fe}_{0.95}\text{Ni}_{0.05})_2\text{As}_2$  crystals. (b) The field-cooled (FC), zero-field-cooled (ZFC) and remanent (REM) susceptibility exhibit a sharp change at the transition temperature ( $T_c = 25$  K and 20 K). (c) “narrow Drude” contribution to dc resistivity plotted as a function of  $T^2$ , as obtained by decomposition  $\rho_N(T) = [\sigma_{\text{total}}(T) - \sigma_B]^{-1}$ , where the  $\sigma_B$  is constant in temperature. The data is presented in arbitrary units since  $\text{Ba}(\text{Fe}_{0.86}\text{Co}_{0.14})_2\text{As}_2$  and  $\text{Ba}(\text{Fe}_{0.816}\text{Co}_{0.184})_2\text{As}_2$  are taken from Ref. 9 where no absolute values are given. (d) Temperature dependence of the scattering rate  $1/\tau_N(T)$  obtained from the fit of the low-frequency optical data by the Drude model.

tion that the effective Umklapp scattering is comparable to the Fermi energy. Furthermore other iron-pnictides behave in a very similar way, as demonstrated on  $\text{Ba}(\text{Fe}_{0.95}\text{Ni}_{0.05})_2\text{As}_2$  in Fig. 3(c), confirming our general view. Notably, a  $T^2$  behavior of the resistivity is also found in 1111 compounds [23, 24]. We note that our discovery of a hidden Fermi-liquid behavior of the governing charge carriers is at variance with previously reported findings. Those works analyzed the resistivity prior to its decomposition, having both contributions,  $\sigma_N(T)$  and  $\sigma_B$ , mixed. The “anomalous” temperature dependence of the resistivity ( $\rho_0 + AT^n$  or  $\rho_0 + AT + BT^2$ ) and the proximity of the magnetic phase have been considered as an indication that the superconducting ground state is a consequence of underlying quantum criticality [9, 10, 20]. Indeed as shown in Fig. 3(a) the total resistivity is clearly not quadratic in temperature and can be well fitted with  $AT^n$  with  $n = 1.25$  for  $\text{Ba}(\text{Fe}_{0.92}\text{Co}_{0.08})_2\text{As}_2$  and  $n = 1.5$  for  $\text{Ba}(\text{Fe}_{0.95}\text{Ni}_{0.05})_2\text{As}_2$ . Only when the incoherent part, determined by optical conductivity, is subtracted, the  $T^2$  law appears in both samples, as demonstrated in Fig. 3(c). With doping the dc resistivity gets considerably smaller [22, 25], because  $\sigma_n$  grows. Consequently the contribution of the incoherent term to  $\sigma_{\text{total}}$  becomes less important. This explains the change in the overall power-law coefficient upon dop-

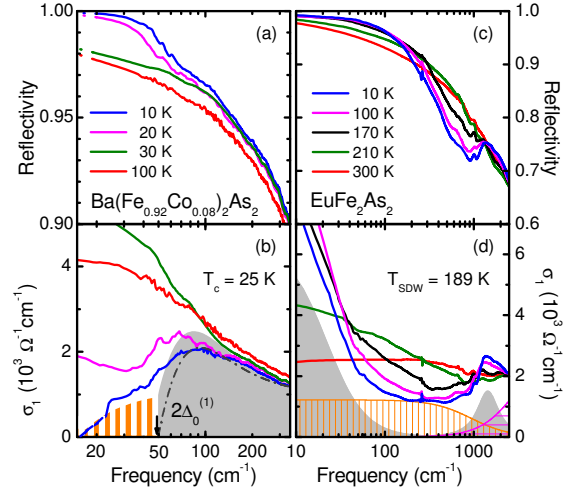


FIG. 4: (Color online) Reflectivity and conductivity of  $\text{Ba}(\text{Fe}_{0.92}\text{Co}_{0.08})_2\text{As}_2$  and  $\text{EuFe}_2\text{As}_2$  above and below the superconducting and SDW transitions. (a) The way the reflectivity of  $\text{Ba}(\text{Fe}_{0.92}\text{Co}_{0.08})_2\text{As}_2$  approaches unity is indicative for the development of the superconducting gap. The dotted lines corresponds to the extrapolations. (b) The optical conductivity  $\sigma_1(\omega, T)$  is gradually depleted up to approximately  $150 \text{ cm}^{-1}$ . The dash-dotted curve is calculated for the lowest temperature assuming one gap  $2\Delta_0^{(1)} = 50 \text{ cm}^{-1}$  and the shaded area by assuming gaps  $2\Delta_0^{(1)} = 50 \text{ cm}^{-1}$  in the  $\sigma_N(\omega)$  component (mainly grey area) and  $2\Delta_0^{(2)} = 17 \text{ cm}^{-1}$  in the  $\sigma_B(\omega)$  background (mainly orange area). (c,d) For  $T < T_{\text{SDW}}$ , a gap in the excitation spectrum of  $\text{EuFe}_2\text{As}_2$  opens. Part of the spectral weight of  $\sigma_N$  shifts from low-frequencies to above approximately  $1000 \text{ cm}^{-1}$ ; but a small Drude-like peak remains. The incoherent background  $\sigma_B(\omega)$  remains basically temperature independent. The fit by the Drude-Lorentz model corresponds to  $T = 10$  K.

ing [25], eventually leading to  $n = 2$ . Our decomposition of the optical conductivity and dc resistivity holds for all analyzed 122 iron-pnictides and reveals the Fermi liquid behavior in  $\sigma_n$ . This result is universal and physically transparent [20]. Next we analyze the superconducting state in detail. Upon passing the superconducting transition the reflectivity of  $\text{Ba}(\text{Fe}_{0.92}\text{Co}_{0.08})_2\text{As}_2$  increases considerably below  $70 \text{ cm}^{-1}$ , as can be seen in Fig. 4(a); for  $\text{Ba}(\text{Fe}_{0.95}\text{Ni}_{0.05})_2\text{As}_2$  a similar behavior is observed around  $60 \text{ cm}^{-1}$ . The way it approaches unity with a change in curvature causes a gap-like structure in the optical conductivity below  $100 \text{ cm}^{-1}$  [Fig. 4(b)]. The removal of spectral weight in  $\sigma_1(\omega, T)$  compared to the normal state conductivity  $\sigma^{(n)}(\omega, T \approx 30 \text{ K})$  extends all the way up to approximately  $150 \text{ cm}^{-1}$ . From the missing area [19],  $A = \int [\sigma_1^{(n)}(\omega) - \sigma_1^{(s)}(\omega)] d\omega$  we estimate the penetration depth to  $\lambda = c/\sqrt{8A} = (3500 \pm 350) \text{ \AA}$  and  $(3000 \pm 300) \text{ \AA}$  for the Co and Ni compounds, respectively. Notably, both materials obey the universal scaling relation of the superfluid density  $\rho_s \propto A$  and the transition temperature  $T_c$  [26, 27]. This indicates that the main

features of the superconducting state are well captured by the optical conductivity. To get further insight, we model our spectra by the BCS-theory for the frequency and temperature dependent conductivity [28]. As seen by the dash-dotted lines in Fig. 4(b), a decent description is obtained with gap value of  $50 \text{ cm}^{-1}$ . Following the suggestions of two isotropic gaps [21, 29, 30], both opening simultaneously below  $T_c$ , we obtain an even better description with  $2\Delta_0^{(1)} = 50 \text{ cm}^{-1}$  in the narrow Drude term only, and a second smaller gap  $2\Delta_0^{(2)} = 17 \text{ cm}^{-1}$  which affects the broad background [31]. Similarly, the description of  $\text{Ba}_{0.6}\text{K}_{0.4}\text{Fe}_2\text{As}_2$  [18] suggests two superconducting gaps. This indicates that the hole-doped iron-pnictides behave in the same way as the electron-doped compounds and that our conclusions are universal in this sense. The gap values obtained from our study are  $2\Delta_0^{(1)}/k_B T_c = 2.5 - 3$ , and 1 for the small gap. ARPES experiments on the K doped compound yield to higher gap values of  $2\Delta_0^{(1)}/k_B T_c = 6.8$  and  $2\Delta_0^{(2)}/k_B T_c < 3$  [21]. It is worthwhile to recall the situation of the two-gap superconductor  $\text{MgB}_2$ , for which several methods evidence two gaps, while far-infrared measurements see only one. By now it is not understood why the optical results agree better with the smaller gap value, although they should be sensitive only to the large one [32]. Due to the proximity of the superconductivity and magnetic ground state it is instructive to compare our results with those obtained on parent compounds. Upon passing through the SDW transition of  $\text{EuFe}_2\text{As}_2$ , for instance [14], a gap in the excitation spectrum opens since parts of the Fermi surface are removed. Importantly, as demonstrated in Fig. 4(d), only spectral weight of  $\sigma_N$  shifts from low-frequencies to above approximately  $1000 \text{ cm}^{-1}$ . The incoherent background  $\sigma_B$  remains basically unchanged. A small Drude-like peak (accounting for the metallic dc properties) remains and becomes very narrow as  $T$  is reduced. On the other hand, the metallic state of the  $\text{Ba}(\text{Fe}_{1-x}\text{M}_x)_2\text{As}_2$  compounds ( $M = \text{Co}$  or  $\text{Ni}$ , close to optimally doping) does not exhibit any trace of the SDW pseudogap (Fig. 1). Upon cooling down to the superconducting transition,  $\sigma_N(\omega)$  gradually narrows and grows [Fig. 1(b,d)]. Importantly, at  $T_c$  a dominant superconducting gap develops in  $\sigma_N$ , i.e. it is associated with the same parts of the Fermi surface gaped by the SDW in parent compounds. Our analysis of the optical conductivity in the normal and broken-symmetry ground states of iron-pnictides, reveals two sorts of conduction electrons associated with  $\sigma_B$  and  $\sigma_N$  (Fig. 2). The broad term  $\sigma_B$  is temperature independent. We ascribe it to an incoherent subsystem which seems to be a common fact in all iron-pnictides. The narrow Drude-like contribution  $\sigma_N$  dominates the conduction in the pnictides. It reveals a  $T^2$  behavior in the resistivity and scattering rate, inferring that superconductivity grows out of a Fermi liquid. Furthermore the dominant gap

at  $2\Delta^{(1)}$  in electron doped  $\text{Ba}(\text{Fe}_{1-x}\text{M}_x)_2\text{As}_2$  and the SDW gap in parent compound  $\text{EuFe}_2\text{As}_2$  develop in  $\sigma_N$ , which signifies that the underlying ground states of iron-pnictides involve the same parts of the Fermi surface. We acknowledge the help of J. Braun and E.S. Zhukova. N.B. is supported by the Alexander von Humboldt Foundation. N.D. thanks the Magarete-von-Wrangell-Programm. The is supported by NSF of China.

- 
- [1] M. R. Norman, *Physics*, 21 (2008).
  - [2] K. Ishida *et al.*, *J. Phys. Soc. Jpn.* **78**, 062001 (2009).
  - [3] J. Dong *et al.*, *Europhys. Lett.* **83**, 27006 (2008).
  - [4] D. J. Singh, *Phys. Rev. B* **78**, 094511 (2008).
  - [5] M. Rotter *et al.*, *New J. Phys.* **11**, 025014 (2009).
  - [6] A. S. Sefat *et al.*, *Phys. Rev. Lett.* **101**, 117004 (2008).
  - [7] L. J. Li *et al.*, *New J. Phys.* **11**, 025008 (2009).
  - [8] F. L. Ning *et al.*, *J. Phys. Soc. Jpn.* **78**, 013711 (2009); F. L. Ning *et al.*, *Phys. Rev. B* **79**, 140506 (2009).
  - [9] J.-H. Chu *et al.*, *Phys. Rev. B* **79**, 014506 (2009).
  - [10] M. Gooch *et al.*, *Phys. Rev. B* **79**, 104504 (2009).
  - [11] N. Barišić *et al.*, *Phys. Rev. B* **78**, 054518 (2008).
  - [12] W. Z. Hu *et al.*, *Phys. Rev. Lett.* **101**, 257005 (2008).
  - [13] M. Nakajima *et al.*, *Physica C* (2009), doi:10.1016/j.physc.2009.11.071
  - [14] D. Wu *et al.*, *Phys. Rev. B* **79**, 155103 (2009).
  - [15] G. Li *et al.*, *Phys. Rev. Lett.* **101**, 107004 (2008).
  - [16] Z. G. Chen *et al.*, *Phys. Rev. B* **80**, 094506 (2009).
  - [17] J. Yang *et al.*, *Phys. Rev. Lett.* **102**, 187003 (2009).
  - [18] W. Z. Hu *et al.*, *Physica C* **469**, 545 (2009).
  - [19] M. Dressel and G. Grüner, *Electrodynamics of Solids* (Cambridge University Press, Cambridge, 2002).
  - [20] Other decompositions of the optical conductivity than suggested here might be tempting, too. For example, the next simplest one is to fit the low-frequency conductivity by a Drude and a Lorentzian terms. However, there is not really any physical meaning of the Lorentzian, and furthermore its position, width and amplitude strongly change with temperature which is highly anomalous.
  - [21] D. V. Evtushinsky *et al.*, *New J. Phys.* **11**, 055069 (2009); V. B. Zabolotnyy *et al.*, *Nature* **457**, 569 (2009).
  - [22] F. Rullier-Albenque *et al.*, *Phys. Rev. Lett.* **103**, 057001 (2009).
  - [23] A. S. Sefat *et al.*, *Phys. Rev. B* **77**, 174503 (2008).
  - [24] S. Suzuki *et al.*, arXiv:0910.1711
  - [25] S. Kasahara *et al.*, arXiv:0905.4427.
  - [26] C. C. Homes *et al.*, *Nature* **430**, 539 (2004).
  - [27] D. Wu *et al.*, *Physica C* (2009), doi:10.1016/j.physc.2009.10.142.
  - [28] D. Mattis and J. Bardeen, *Phys. Rev.* **111**, 412 (1958).
  - [29] R. Khasanov *et al.*, *Phys. Rev. Lett.* **102**, 187005 (2009).
  - [30] I. I. Mazin *et al.*, *Phys. Rev. Lett.* **101**, 057003 (2008); I. I. Mazin and J. Schmalian, *Physica C* **469**, 614 (2009).
  - [31] The single-gap model significantly deviates from the data in the range of high accuracy between 100 and  $300 \text{ cm}^{-1}$ , because the incoherent  $\sigma_B$  has a large width. The hatched area in Fig. 4(b) indicates the superior description by the two-gap BCS model; it does not imply an unambiguous proof of its size. The experimental results for  $\text{Ba}(\text{Fe}_{0.95}\text{Ni}_{0.05})_2\text{As}_2$  are qualitatively identical, but with a

lower value  $2\Delta_0^{(1)} = 35 \text{ cm}^{-1}$  in the narrow Drude term. The small gaps fall below the range in which reliable data could be acquired.

[32] A.B. Kuzmenko, *Physica C* **456**, 63 (2007) and references therein.